

Optically Powered and Controlled Drones Using Optical Fibers for Airborne Base Stations

Natsuki Shindo ¹, Taiki Kobatake ¹, Denis Masson ², Simon Fafard ² and Motoharu Matsuura ^{1,*} 

¹ Graduate School of Informatics and Engineering, University of Electro-Communications, 1-5-1 Chofugaoka, Chofu, Tokyo 182-8585, Japan

² Broadcom, IFPD Division, Ottawa, ON K1A 0R6, Canada

* Correspondence: m.matsuura@uec.ac.jp

Abstract: Mobile communication services are crucial during emergency disasters and temporary events, and future mobile communication systems should be able to provide such services. Airborne base stations using drones are highly effective as stand-in base stations in areas where the ground base stations are inoperable or at temporary event sites. However, it is difficult for conventional drones to provide mobile communication services without interruption due to flight time limitations caused by their limited battery capacity. Thus, a drone drive with a non-interrupted power supply is urgently needed. In this study, we developed an airborne base station that enables drones to be driven and maneuvered by optical fibers. We simultaneously transmitted radio frequency (RF) data signals for the airborne base station and control signals for the drone and evaluated the transmission performances of the RF signals and the controllability of the drone. Furthermore, we conducted a flight experiment on a medium-sized drone powered by optical fibers.

Keywords: power over fiber; radio-over-fiber; airborne base stations; drone; mobile communications



Citation: Shindo, N.; Kobatake, T.; Masson, D.; Fafard, S.; Matsuura, M. Optically Powered and Controlled Drones Using Optical Fibers for Airborne Base Stations. *Photonics* **2022**, *9*, 882. <https://doi.org/10.3390/photonics9110882>

Received: 31 October 2022

Accepted: 18 November 2022

Published: 21 November 2022

Publisher's Note: MDPI stays neutral with regard to jurisdictional claims in published maps and institutional affiliations.



Copyright: © 2022 by the authors. Licensee MDPI, Basel, Switzerland. This article is an open access article distributed under the terms and conditions of the Creative Commons Attribution (CC BY) license (<https://creativecommons.org/licenses/by/4.0/>).

1. Introduction

Recently, mobile communication has become an indispensable facet of everyday life. Ground base stations have been installed worldwide to facilitate mobile communications services everywhere. However, there are increasing demands for airborne base stations that provide temporary mobile communication services [1–3]. For example, an alternative base station would be urgently needed after the collapse of a ground base station due to natural disasters, such as a big earthquake or typhoon. In such situations, portable airborne base stations can be deployed in disaster areas to provide temporary mobile services. Moreover, airborne base stations can be used to provide mobile communication services to numerous mobile users during planned temporary events, such as outdoor concerts or sports competitions, where numerous mobile users are concentrated.

Currently, drones are the most promising airborne base stations [4,5]. Drones are compact and lightweight, making them easy to carry, and they require little space for takeoff or landing. However, when used as an airborne base station, their battery capacity limits the flight time, hindering continuous mobile services over long durations. Additionally, the onboard battery accounts for most of the total weight of the drone, which increases power consumption and is a major limiting factor for its payload.

Therefore, it is necessary to develop a drone charging technology that does not require large-capacity batteries without time limitations. The most popular method is a wired power supply using metal power lines. Despite some commercialization [6,7], there are risks of electric shocks, lightning damage, and radio frequency (RF) interference when used as an airborne base station. Drones that are powered wirelessly via microwaves [8] or lasers [9,10] do not require power lines. However, a beam-tracking function is required, and high-power energy is radiated into space, posing a safety hazard. Thus, we developed an optically powered drone using a power-over-fiber (PWoF) and successfully demonstrated

a flight experiment using an entry-size drone [11]. PWoF is an established and practical technology that enables power transmission over lightweight, non-conductive glass fiber lines [12,13]. Recently, simultaneous electric power exceeding 40 W, along with optical data signals, has been reported [14]. Furthermore, because airborne base stations need to communicate wirelessly with multiple mobile terminals, it is preferable to use radio-over-fiber (RoF) to maneuver drones instead of wireless communication to prevent RF signal interference. Thus far, we have simultaneously transmitted RF data signals for airborne base stations in mobile communications and control signals for maneuvering drones over optical fibers [15]. However, actual drone control has not yet been achieved.

Herein, we presented an optically powered and controlled drone with optical fibers for airborne base stations. In order to demonstrate the feasibility of the drone, we transmitted RF data signals to the airborne base station and controlled signals to maneuver the drone simultaneously. Moreover, we evaluated the transmission performance and confirmed the controllability of the drone using RoF transmission when the wireless control signal is disconnected. Additionally, we conducted a flight experiment on a medium-sized drone driven only by the PWoF. This drone was much larger than that used in our previous experiments.

The remainder of this paper is organized as follows. In Section 2, we introduced the concept and features of optically powered and controlled drones using optical fibers. Section 3 evaluates the transmission performance of the RF data signal and control signal over an optical fiber link connecting the ground station facility and the drone. In Section 4, we confirmed the controllability of an optically controlled drone using the RoF transmission. Section 5 describes the flight experiment of a medium-sized drone. After discussing the future challenges and prospects of optically powered and controlled drones for airborne base stations in Section 5, we concluded the paper in Section 6.

2. Optically Powered and Controlled Drone Using Optical Fibers

Figure 1a shows a schematic view of an optically powered and controlled drone for an airborne base station. The drone and ground station facility is connected by two optical fibers, assuming a standard single-mode fiber (SSMF) for RF data and control signal transmission and a multi-mode fiber (MMF) with a large core diameter for PWoF. The maximum transmission distance of the optical fiber is assumed to be approximately 100 m. If an RF data signal with a carrier frequency in the several GHz band can output the signal power of approximately 10 W, mobile communications can be performed in an area with a maximum cell radius of 5–10 km if the line-of-sight is adequate.

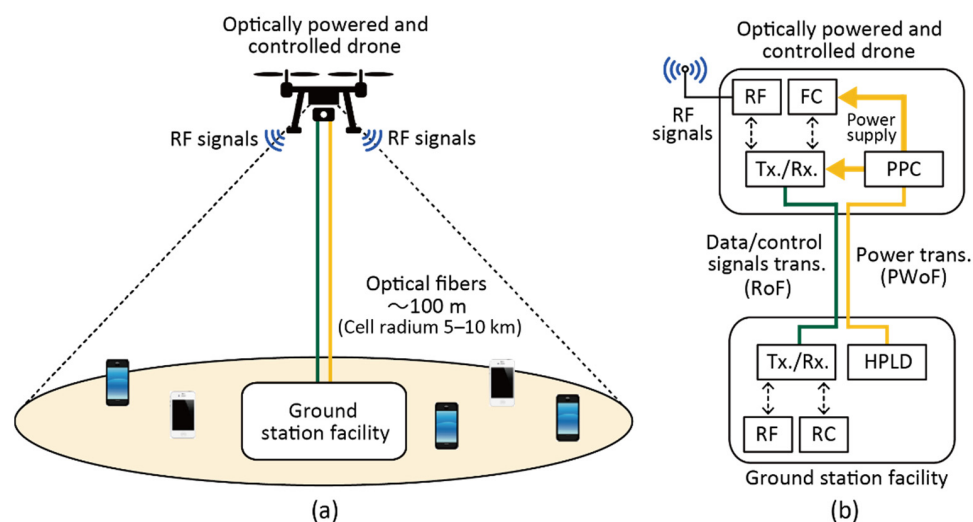


Figure 1. (a) Schematic view and (b) configuration of optically powered drone using optical fibers for airborne base stations. FC: flight controller, PPC: photovoltaic power converter, RC: remote controller, HPLD: high-power laser diode.

The configuration of optically powered and controlled drones is shown in Figure 1b. In the ground station facility, the RF data signals for the airborne base station and the control signals generated by a remote controller for maneuvering the drone were converted into optical signals and transmitted into the SSMF as RoF signals. At the airborne base station, the RF data signals are radiated from the antenna, and the control signals are input to the flight controller (FC), which is used to maneuver the drone. The system was designed to support bidirectional transmission. The power required to drive the drone was provided by a high-power laser diode (HPLD) deployed at the ground station facility. The feed light generated by the HPDL is transmitted to an MMF and converted into electric power using a photovoltaic power converter (PPC). The converted electric power is used to drive the transmitter, receiver, and FC. It should be noted that multiple HPLDs, optical fibers, and PPCs are required as the supplied power increases. The ground station facility and the airborne base station are connected only by optical fibers, which are non-conductive lines; thus, in the event of a lightning strike near the airborne base station, no dangerous current back to the ground station facility is possible. Additionally, the RF data and control signals transmitted over the optical fiber are electrically isolated; thus, the RF signals radiated by the antenna are unaffected by electromagnetic induction.

3. Simultaneous RF Data and Control Signal Transmission

In order to evaluate the transmission performances of the RF data and control signals, simultaneous transmission experiments were conducted using a 100 m SSMF; Figure 2 shows the experimental setup. An IEEE802.11g wireless LAN standard, orthogonally frequency division multiplexing (OFDM), and 64-quadrature amplitude modulation (64-QAM) signal were used as an RF data signal. The carrier frequency and bit rate were 5.2 GHz and 54-Mbit/s, respectively. The signal was generated using a signal generator (SG). The drone used in this experiment was a commercially available, small-size, entry-type drone (Hubsan Co. Ltd., Shenzhen, China, H111 Nano Q4). An electrical signal with a carrier frequency of 2.425 GHz was used as the control signal. This signal was generated by the RC attached to the drone used, and the output signal was combined with the RF data signal from an electrical coupler (EC) via an electrical circulator (ECIR). The combined RF data and control signals were converted into an optical analog signal using a laser diode (LD) at a wavelength of 1554 nm for RoF transmission. After amplification by an erbium-doped fiber amplifier (EDFA), the optical analog signal was passed through a bandpass filter (BPF) to eliminate amplified spontaneous emission noise and a circulator (CIR) and was transmitted over a 100 m SSMF. After passing through the CIR, the optical analog signal was converted into an electrical signal by a photodiode (PD), with only the signal modulation component extracted by a bias tee (BT). The RF data signal divided by an EC was evaluated using a signal analyzer (SA) for signal quality evaluation, and the control signal was input to the FC of the drone for drone control. In this experimental setup, the RF data signal was only transmitted downstream, whereas the control signal was transmitted both downstream and upstream. This is because the drone is inoperable without sending a data reception confirmation signal from the FC of the drone to the RC to control it. The data reception confirmation signal was passed through the ECIR and converted into an optical analog signal by an LD at a wavelength of 1549 nm. After two CIR and 100 m SSMF transmissions, the optical signal was converted into an electrical signal and input to the RC. Upon receiving the data confirmation signal from the FC, the RC recognized that the connection state had been secured and could then transmit the control signals necessary to maneuver the drone. In this experiment, the RF data signal is assumed to be transmitted only through downlink transmission. For uplink transmission, the control signal from the FC and an uplink RF data signal must be combined and converted to an optical signal with the 1549 nm LD. Then, the optical data signal must be transmitted over the SSMF.

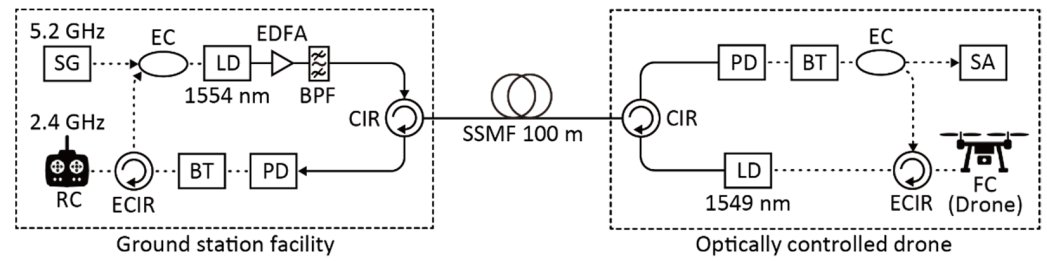


Figure 2. Experimental setup for simultaneous RoF data and control signals transmission for airborne base station. SG: signal generator, RC: remote controller, EC: electrical coupler, ECIR: electrical circulator, LD: laser diode, EDFA: erbium-doped fiber amplifier, BPF: bandpass filter, PD: photodiode, BT: bias tee, CIR: circulator, SA: signal analyzer, FC: flight controller.

Figure 3 shows the electrical spectra of the RF data and control signals transmitted over the 100 m SSMF measured by the SA. In the RF data signal, a high SNR spectrum with a center frequency of 5.2 GHz was observed. A rectangular spectrum, which is characteristic of OFDM signals, is also observed in the spectral waveform. However, a spectral waveform narrower than that of the RF data signal was observed for the control signal with a center frequency of 2.425 GHz. This center frequency was seen to change to a different frequency each time the RC was turned on and off. This was due to the specification for preventing interference with other control signals during wireless operation during conventional outdoor use.

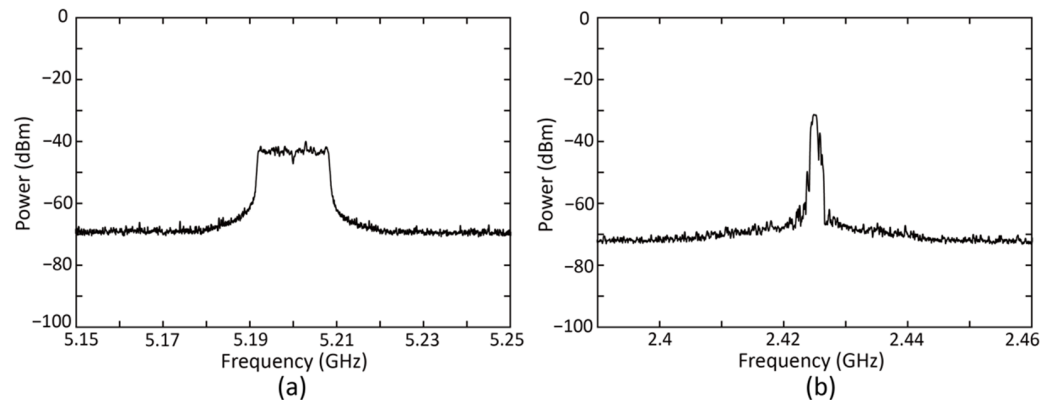


Figure 3. Electrical spectra of (a) RF data and (b) control signals after 100 m SSMF transmission.

For a detailed evaluation of the transmission performance of the RF data signal, the error-vector magnitude (EVM) of the transmitted signal was measured; the results are shown in Figure 4. The dashed line shows an EVM of 5.6%, which is necessary to ensure adequate received signal quality for the modulation format used. The inset shows the constellation of the transmitted RF data signal when the SG output power was 2 dBm. As the SG output power increases above 0 dBm, the EVM value also increases. This was due to the nonlinear distortion caused by the excessive electrical power input to the LD. However, as the SG output power decreased below 0 dBm, the EVM slowly increased. This indicates signal quality degradation due to the weakening of the signal component. In contrast, the EVM was below 5.6% over a very wide power range, indicating that the received RF data signal had high signal quality. The results indicate that the signal transmitted to the drone has a sufficient signal quality to be radiated from the airborne base station.

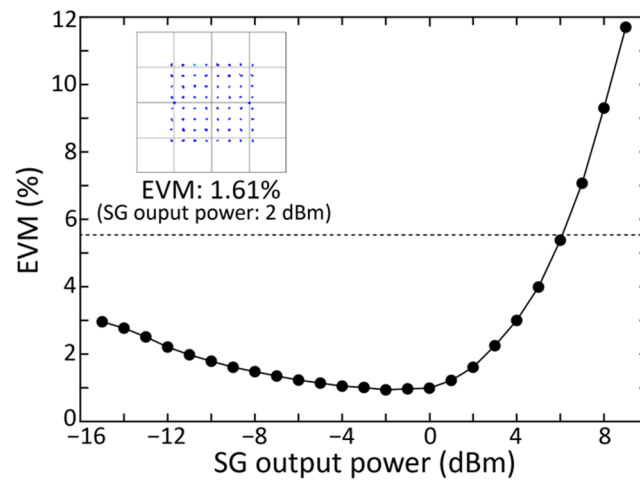


Figure 4. EVM as a function of SG output power. Dashed line shows EVM of 5.6%. Inset shows constellation of transmitted RF data signal when SG output power was 2 dBm.

4. Controllability of the Optically Controlled Drone

In order to verify whether the control signals are accurately transmitted by the RoF transmission, we conducted drone control tests based on the experimental setup shown in Figure 2. First, because the RC and FC of the drone system could transmit and receive even very weak wireless control signals, the drone itself was covered with an RF-absorbing sheet to completely block the wireless control signal. Figure 5a,b show the electrical spectra of the EC output (measured by the SA) in the airborne base station without and with the RF-absorbing sheet, respectively. Here, the LD at the ground station facility was turned off, and no optical signals were transmitted. In Figure 5a, when the RC is turned on, wireless signals are detected in the control signal and other frequency bands. However, in Figure 5b, even if the RC is turned on, the control signals and other RF signal components are undetected. Additionally, the pairing could not be performed via wireless communication when the drone and RC were actually turned on with the RF-absorbing sheet, confirming that the control signals were blocked.

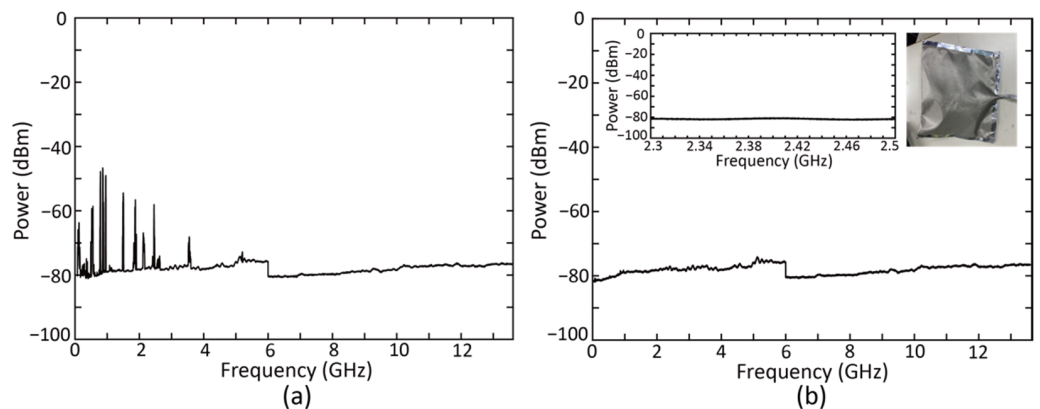


Figure 5. Electrical spectra of EC output (a) without and (b) with RF absorbing sheet. Insets of (b) show electrical spectrum at around center frequency of control signal and photo of RC covered with RF absorbing sheet.

By using the RF-absorbing sheet, we controlled the drone by RoF transmission using a 100 m SSMF, as shown in Figure 2. Photographs illustrating drone control are shown in Figure 6. We confirmed the operability of the drone via the RC controller by performing eight different control operations, wherein the drone initiated pairing operations through RoF transmission. This shows that the drone can be operated using an optical fiber, even without wireless communication.

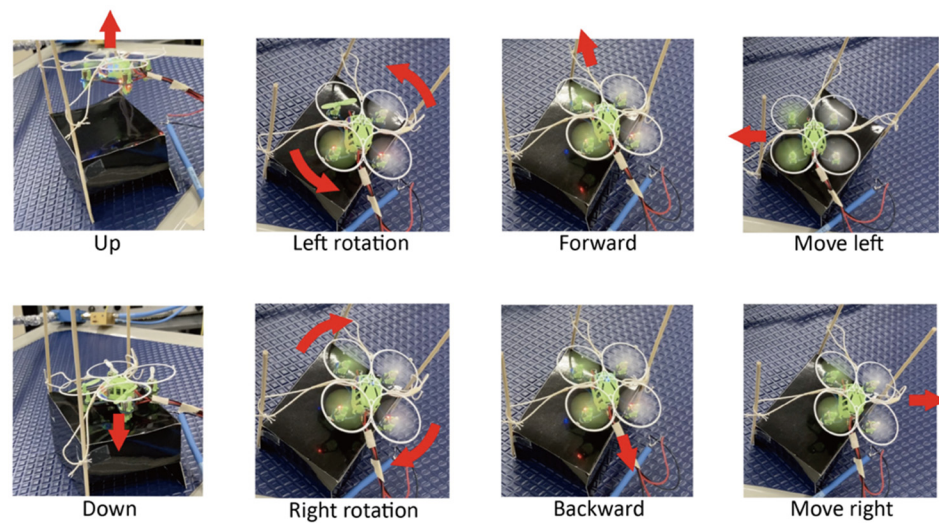


Figure 6. Photographs illustrating control of optically controlled drone. Red arrows indicate direction in which the drone is moving.

5. Flight Demonstration of the Optically Powered Drone

We previously demonstrated the flight experiment of an entry-sized drone using PWoF [11]. However, larger drones must be driven to carry a base station and achieve flight at higher altitudes. In this Section, we demonstrated a flight experiment of a much larger drone than the drone used in the previous study by improving the power transmission performance of the PWoF [16].

5.1. Device Characteristics

There are two key devices for driving a drone with PWoF. One is a PPC, which converts optical power into the electric power required to drive the drone. The other is a DC-DC converter (DDC) that converts the output voltage of the PPC to the voltage required to drive the drone. In this Section, the characteristics of the PPC and the DDC we selected are evaluated prior to the drone flight experiment.

The optical-to-electrical (O/E) power conversion efficiency of the PPC was measured to evaluate whether the PPC we used could supply the power necessary to drive the drones. Figure 7 shows the experimental setup used for the measurements. We used a commercially available HPLD with a wavelength of 808 nm as a feed light source. The maximum output power and the core diameter of the pigtailed MMF were 40 W and 105 μm , respectively. The MMF used had a core diameter of 105 μm and a length of 100 m, similar to the SSMF used in the RoF transmission. Both ends of the MMF were common fiber connectors (FC/PC connectors), and these connectors connected to the pigtail fiber of the HPLD and the PPC itself. After transmission, the MMF was connected to the PPC, which was a specially customized GaAs-based PPC based on a vertical epitaxial monolithic heterostructure architecture design [14,17,18]. The PPC provides a higher capability both of O/E conversion efficiency and available input optical power than conventional PPCs. An electronic load device was connected to the output of the PPC, and the characteristics of the PPC were measured when the resistance of the load was varied.

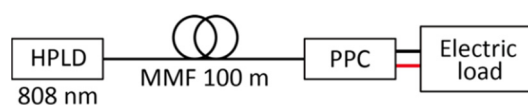


Figure 7. Experimental setup for O/E conversion performance measurement of PPC.

Figure 8a,b shows the current–voltage (I–V) and power–voltage (P–V) curve characteristics of the PPC while changing the input optical power, respectively. As the input optical power increases up to 25 W, the current and converted electric power are increased.

However, for all input optical powers, the current and electrical power decreased rapidly when a certain voltage value was reached. This voltage is called the maximum power point (MPP), which is approximately 6.2 V for the PPC. In the 25 W optical power injection, the electric power of 14 W could be obtained at the MPP.

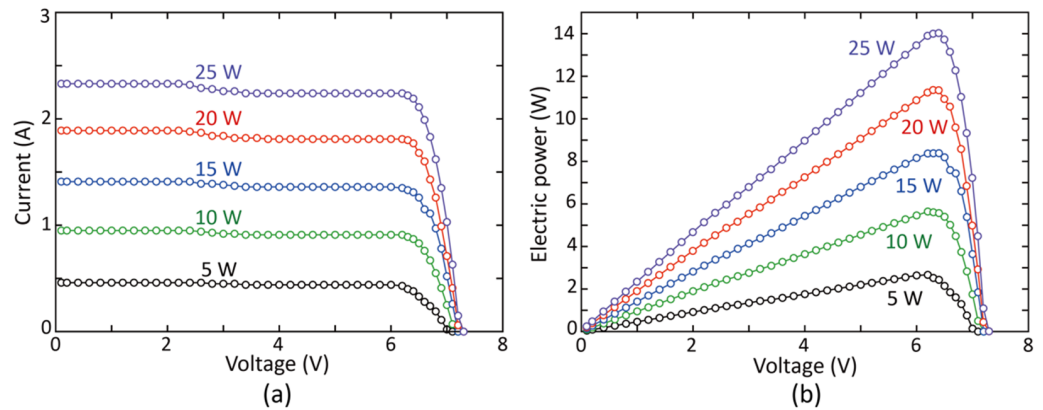


Figure 8. (a) IV and (b) PV curve characteristics of PPC while changing input optical power.

In order to drive a drone by PWoF, it is important not only to input a higher optical power to the PPC but also to adjust the voltage between the PPC output and the drone input after converting it to electric power. The power consumption of the drone used in this experiment was 10.4 to 12.6 W. In the original drone, the power was supplied by a 1-cell LiPo battery, which had an allowable voltage range of 3.0 to 4.1 V. On the other hand, the voltage at which MMP is achieved in the PPC was 6.2 V. Since it would exceed the allowable voltage if it is directly connected, it is necessary and beneficial to use a DDC to match the voltage required for the drone.

Figure 9 shows the conversion efficiency of three commercially available DDCs (DDC-A: Murata Co. Ltd., OKL-T/6-W12N-C, DDC-B: XLSEMI, XL4015, DDC-C: Sanken Electric Co. Ltd., SI-8008HFE) for various currents. In this measurement, the output voltage was set to 3.7 V, which is optimal for driving the drone. The current increases rapidly up to around 0.5 A and then tends to remain almost constant or decrease slowly. Of the three converters, DDC-A had the highest conversion efficiency at all the currents. Therefore, the device was used in the following drone flight demonstration.

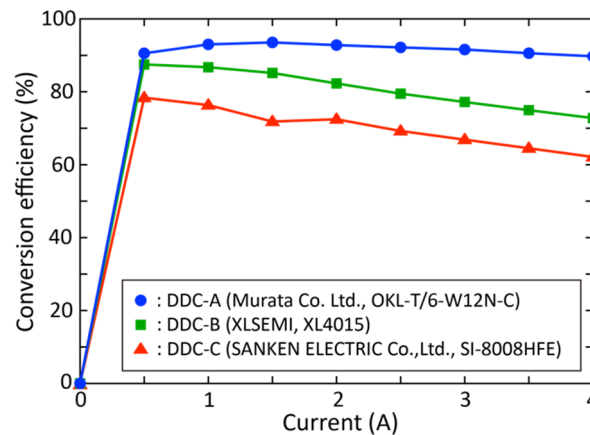


Figure 9. Conversion efficiency of three commercially available DDCs for various currents.

5.2. Flight Demonstration

We conducted a flight experiment using a commercially available drone. Figure 10a shows the experimental setup. As shown in Figure 7, the output of the HPLD at 808 nm was connected to the 100 m MMF and converted to electrical power at the PPC. The output

voltage from the PPC was converted to 3.7 V using DDC-A to obtain the optimum voltage for the drone. The transmission loss of the 100 m MMF was 1.2 dB. The input optical power to the PC and the O/E conversion efficiency was 25 W and 56%, respectively. The drone used in this experiment was a commercially available, medium-sized drone (FUGU INNOVATIONS Co. Ltd., Yokohama, Japan, SMAO S5). The battery of the drone was removed during the PWoF operation, as it was not required. This reduced the weight of the drone from 100 g to 76.7 g. It should be noted that only the drone was flown, as the PPC and DDC-A could not be mounted. Furthermore, in this experiment, the drone was not optically controlled by RoF transmission but by wireless control signals using the attached RC.

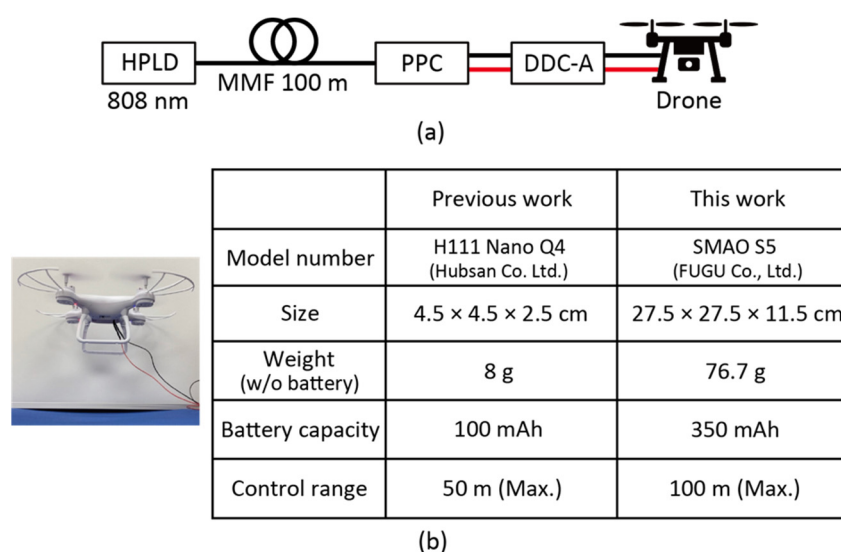


Figure 10. (a) Experimental setup for drone flight demonstration. (b) Photograph of drone flight demonstration and basic specification of drones used in a previous study and this study.

Figure 10b shows a photograph of the flight demonstration of the drone and the basic specifications of the drones used in the previous study and this study. By increasing the supplied power using the PPC and DDC-A, we successfully flew a drone that was approximately 10 times heavier and 36 times larger than previously [11]. Moreover, the operable control range was extended to 100 m, which is assumed to be the operating range for airborne base stations.

6. Discussion

In this study, we demonstrated optically powered and controlled drones using optical fiber and a flight experiment of a medium-sized drone using a PWoF. However, there are significant challenges in actually driving a drone that functions as an airborne base station using only the PWoF. Figure 11 shows the relationship between the takeoff weight and the power consumption of commercially available drones, as indicated by the circles. In order to transmit and receive RF data signals for an airborne base station along with control signals to maneuver the drone, the drone must be mounted with the necessary components in the airborne base station, as shown in Figure 2, and the airborne base station itself. Although airborne base stations have rapidly become lighter in recent years, these components as a whole are expected to weigh from several hundred grams to 1 kg. In addition to these components, a DDC and PPC must be mounted to drive the drone with PWoF, as shown in Figure 10a. Therefore, we assume that the total takeoff weight of a drone that functions as an airborne base station is at least approximately 1 kg. As shown in Figure 11, the relationship between the takeoff weight and power consumption of commercially available drones can be approximately fitted by a linear approximation, as indicated by the red line. It can be seen that the highest takeoff weight on a commercially

available drone requires more than 100 W of power. Therefore, although power saving by drones can be expected, flying a drone that functions as an airborne base station requires approximately 10 times more power than the current power supply capability. In order to achieve this, it is necessary to increase the power supply by installing multiple HPLDs, optical fibers, and PPCs for the PWoF.

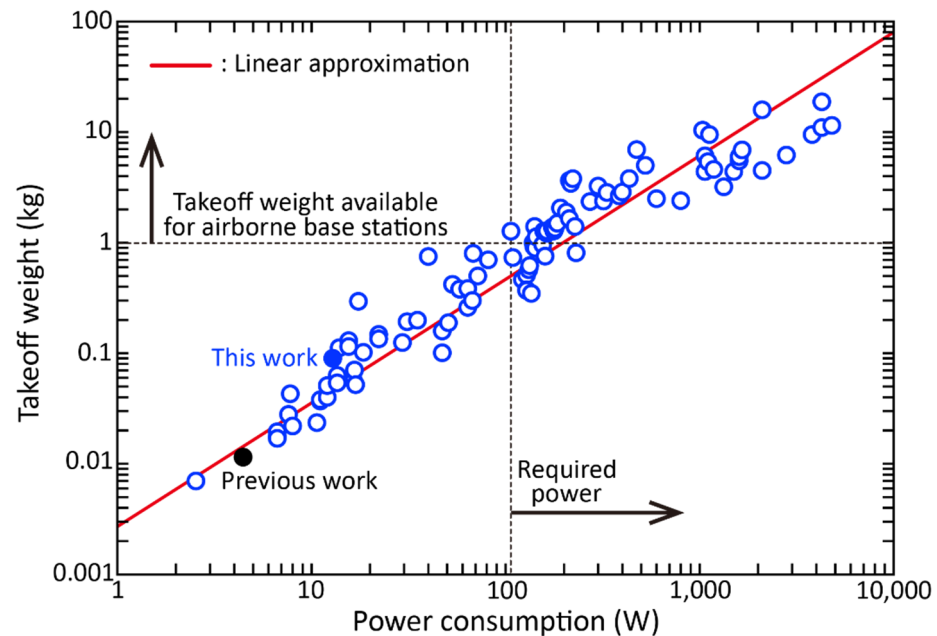


Figure 11. Takeoff weight versus power consumption of commercially available drones. Dashed lines show thresholds of takeoff weight and required power available for airborne base stations.

The effect of weather on the use of drones as airborne base stations is also discussed. In rainy or snowy weather, waterproofing must be deployed on the drone because there is a high chance of a short circuit occurring in its electrical components. In addition, temperature also has a significant impact on drones. In particular, many drones currently use lithium polymer batteries, which have an optimal operating temperature of 40 °C. Therefore, the battery performance will be greatly reduced at high altitudes and in cold climates [19,20]. In contrast, optically powered and controlled drones are not equipped with batteries, and their fiber-optic components and PPCs are resistant to low-temperature environments. Therefore, the more stable operation will be expected at high altitudes and in cold climates compared to conventional drones with batteries.

7. Conclusions

We presented an optically powered and controlled drone using optical fibers for airborne base stations. In order to demonstrate the feasibility of the drone, we experimentally transmitted RF data signals for the airborne base station and control signals to maneuver the drone simultaneously. We obtained high transmission performance of the RF data signals and good controllability of the control signals when the wireless control signal was disconnected. We also demonstrated a flight experiment on a medium-sized drone driven only by PWoF, which was approximately 10 times heavier and 36 times larger than that of our previous study. Although additional power is required to drive a drone carrying an actual airborne base station using only PWoF, the results obtained in this study will be useful for realizing optically powered and controlled drones that can function as airborne base stations.

Author Contributions: Conceptualization and methodology, M.M., N.S., D.M. and S.F.; investigation, N.S. and T.K.; data curation, N.S.; writing—original draft preparation, M.M.; writing—review and editing, M.M., D.M. and S.F. All authors have read and agreed to the published version of the manuscript.

Funding: This research received no external funding.

Institutional Review Board Statement: Not applicable.

Informed Consent Statement: Not applicable.

Data Availability Statement: Not applicable.

Conflicts of Interest: The authors declare no conflict of interest.

References

1. Frew, E.W.; Brown, T.X. Airborne communication networks for small unmanned aircraft systems. *Proc. IEEE* **2008**, *96*, 2008–2027. [[CrossRef](#)]
2. Goddemeier, N.; Daniel, K.; Wietfeld, C. Role-based connectivity management with realistic air-to-ground channels for cooperative UAVs. *IEEE J. Sel. Areas Commun.* **2012**, *30*, 951–963. [[CrossRef](#)]
3. Zeng, Y.; Zhang, R.; Lim, T.J. Wireless communications with unmanned aerial vehicles: Opportunities and challenges. *IEEE Commun. Mag.* **2016**, *54*, 36–42. [[CrossRef](#)]
4. Naqvi, S.A.R.; Hassan, S.A.; Pervaiz, H.; Ni, Q. Drone-aided communication as a key enabler for 5G and resilient public safety networks. *IEEE Commun. Mag.* **2018**, *56*, 36–42. [[CrossRef](#)]
5. Dao, N.-N.; Pham, Q.-V.; Tu, N.H.; Thanh, T.T.; Bao VN, Q.; Lakew, D.S.; Cho, S. Survey on aerial radio access networks: Toward a comprehensive 6G access infrastructure. *IEEE Commun. Surveys Tut.* **2021**, *23*, 1193–1225. [[CrossRef](#)]
6. Elistair Inc. The Tethered Drone Company. Available online: <https://elistair.com> (accessed on 12 October 2022).
7. Aerosense Inc. Cutting Edge Drone, Ai, and Cloud Technology. Available online: <https://aerosense.co.jp/english> (accessed on 12 October 2022).
8. Moro, R.; Keicho, N.; Motozuka, K.; Matsukura, M.; Shimamura, K.; Fukunari, M.; Mori, K. 28 GHz microwave power beaming to a free-flight drone. In Proceedings of the IEEE Wireless Power Transfer Conference, WPTC 2021, San Diego, CA, USA, 1–4 June 2021; pp. 1–4.
9. Zhang, J.; Miyamoto, T. Investigation of flying condition of small drone powered by optical wireless power transmission using VCSEL. In Proceedings of the 4th Optical Wireless and Fiber Power Transmission Conference, OWPT 2020, Online, Japan, 21–23 April 2020; p. OWPT7-02.
10. Kikuchi, Y.; Miyamoto, T. Design and characterization of dynamic OWPT charging to micro-drones. In Proceedings of the 4th Optical Wireless and Fiber Power Transmission Conference, OWPT 2022, Yokohama, Japan, 18–21 April 2022; p. OWPT5-02.
11. Yazawa, R.; Matsuura, M. Optically powered drone small cells using optical fibers. *IEICE Electron. Express* **2018**, *15*, 20180371.
12. Matsuura, M. Recent advancement in power-over-fiber technologies. *Photonics* **2021**, *8*, 335. [[CrossRef](#)]
13. Matsuura, M. Power-over-fiber using double-clad fibers. *IEEE J. Lightwave Technol.* **2022**, *40*, 3187. [[CrossRef](#)]
14. Matsuura, M.; Nomoto, H.; Mamiya, H.; Higuchi, T.; Masson, D.; Fafard, S. Over 40-W electric power and optical data transmission using an optical fiber. *IEEE Trans. Power Electron.* **2021**, *36*, 4532–4539. [[CrossRef](#)]
15. Kobatake, T.; Shindo, N.; Matsuura, M. Simultaneous fiber transmission of control and mobile communication signals in power-over-fiber drones for airborne base stations. In Proceedings of the 3rd Optical Wireless and Fiber Power Transmission Conference, OWPT 2021, Online, 19–22 April 2021; p. OWPTp-01.
16. Shindo, N.; Kobatake, T.; Matsuura, M.; Masson, D.; Fafard, S. Flight demonstration of power-over-fiber drone for aerial base stations. In Proceedings of the 4th Optical Wireless and Fiber Power Transmission Conference, OWPT 2022, Yokohama, Japan, 18–21 April 2022; p. OWPTp-01.
17. Fafard, S.; York, M.C.A.; Proulx, F.; Valdivia, C.E.; Wilkins, M.M.; Arès, R.; Aimez, V.; Hinzer, K.; Masson, D.P. Ultrahigh efficiencies in vertical epitaxial heterostructure architectures. *Appl. Phys. Lett.* **2016**, *108*, 071101. [[CrossRef](#)]
18. Fafard, S.; Masson, D.; Werthen, J.G.; Liu, J.; Wu, T.C.; Hundberger, C.; Schwarzfischer, M.; Steinle, G.; Gaertner, C.; Piemonte, C.; et al. High performance laser power converters and applications. In Proceedings of the 4th Optical Wireless and Fiber Power Transmission Conference, OWPT 2022, Yokohama, Japan, 18–21 April 2022; p. OWPT1-01.
19. Kim, S.J.; Lim, G.J.; Cho, J. Drone flight scheduling under uncertainty on battery duration and air temperature. *Comput. Ind. Eng.* **2018**, *117*, 291–302. [[CrossRef](#)]
20. Gao, M.; Hugenholtz, C.H.; Fox, T.A.; Kucharczyk, M.; Barchyn, T.E.; Nesbit, P.R. Weather constraints on global drone flyability. *Sci. Rep.* **2021**, *11*, 12092. [[CrossRef](#)] [[PubMed](#)]